JOURNAL OF PROPULSION AND POWER
Vol. 20, No. 6, November–December 2004

Effect of Paramagnetism and Diamagnetism on Theoretical Rocket Performance

John Baker*
The University of Alabama, Tuscaloosa, Alabama 35487-0276
and
Orenthral T. Morgan†
Pratt and Whitney, East Hartford, Connecticut 06108

The impact of an externally applied magnetic field on theoretical rocket performance has been investigated and the results of this investigation are presented and discussed. The application of a magnetic field has been assumed to impact rocket performance as a result of only the paramagnetic and diamagnetic nature of the constituent species in order to isolate the related phenomena. For the results presented in this paper, the impact of an applied magnetic field has been evaluated only for the case of an infinite area combustor. The equilibrium chemical composition produced in the combustor was assumed frozen as the fluid expanded through a supersonic nozzle. The parametric investigation examined a model reaction between kerosene and oxygen. The theoretical model was validated by comparison with existing chemical equilibrium and theoretical rocket performance models for the case of no applied magnetic field. The results indicate that the application of a magnetic field decreases mixture molecular mass, increases specific impulse, decreases the expansion ratio required for isentropic flow, and decreases the thrust coefficient.

Nomenclature

A	=	area
B	=	magnetic induction
C_F	=	thrust coefficient
c_p	=	constant pressure specific heat
c^*	=	characteristic velocity
g	=	acceleration due to gravity
H	=	magnetic field strength
I_s	=	specific impulse
k	=	ratio of specific heats
M_M	=	molecular mass
m	=	mass flow rate
n	=	number of moles
O/F	=	oxygen-to-fuel ratio
p	=	pressure
R_u	=	universal gas constant
T	=	temperature
u	=	fluid speed
V	=	volume
W	=	work
y_i	=	mole fraction of species i
ρ	=	density

Subscripts

e	=	exit conditions
m	=	iteration counter
mix	=	mixture
o	=	stagnation conditions
t	=	throat conditions

Received 19 June 2003; revision received 23 April 2004; accepted for publication 25 April 2004.

*Associate Professor, Department of Mechanical Engineering, Box 870276; John.Baker@coe.eng.ua.edu.
†Aerothermal Engineer, PSA-OSV.

Introduction

MAGNETIC fields are known to influence the performance of propulsion systems as a result of the interaction between the magnetic field and the associated ionized gases, that is, through the Lorentz body force. Many nonconventional propulsion systems employ a magnetic field to accelerate plasma in order to produce thrust.[1–3] For solid rocket motors, the application of an applied magnetic field has been shown to increase the temperature and pressure near the burning surface and thus produce up to a ten-fold increase in the mass burn rate as the result of the interaction between the magnetic field and the ionized combustion gases.[4,5] The interaction between a magnetic field and an ionized gas is not the only way a magnetic field can influence the performance of a chemical rocket. Magnetic fields influence the behavior of all materials as a result of paramagnetism and diamagnetism. Paramagnetism is the weak attraction to a magnetic field experienced by a material composed of atoms with permanent magnetic dipole moments. Because the magnetic dipole moments of a paramagnetic material are randomly oriented, there is an insignificant interaction when no magnetic field is applied. When a magnetic field is applied to such materials, the atoms align with the magnetic field and produce a mild attraction. The strength of this attraction is proportional to the strength of the externally imposed magnetic field. The magnetic behavior associated with the dipole moments in a paramagnetic gas must compete with the randomizing effect of temperature. This behavior is functionally described by the magnetic susceptibility. The magnetic susceptibility is the ratio of the magnetization to the magnetic field strength. In a paramagnetic gas, the magnetic susceptibility is thus a function of temperature. Materials consisting of atoms with no permanent magnetic dipole moments exhibit diamagnetic behavior. When an external magnetic field is applied, the atoms of a diamagnetic material develop a net dipole moment. This induced moment opposes the applied field, and thus a diamagnetic material exhibits a weak repulsion to an applied magnetic field. The repulsion to the magnetic field increases with increasing magnetic field strength. Unlike paramagnetic gases, the magnetic susceptibility of a diamagnetic gas is independent of temperature. For chemical rocket engines, the principal paramagnetic gas is oxygen, whereas most of the other species are diamagnetic.

Although the forces associated with the interaction between magnetic fields and plasmas are orders of magnitude greater than those associated with paramagnetic and diamagnetic interactions, the

highly nonlinear nature of the combustion process in a chemical rocket could potentially be influenced by paramagnetism and diamagnetism. Previous research indicates that under certain conditions applied magnetic fields can significantly impact equilibrium combustion compositions when considering only paramagnetic and diamagnetic behavior.[6] It is not unreasonable to expect that the application of an applied magnetic field would therefore affect theoretical rocket performance as a result of paramagnetic and diamagnetic behavior. For isentropic flow through a nozzle, the speed of the fluid at the nozzle exit can be calculated using[7]

$$u_e = \sqrt{\frac{2k_{\text{mix}} R_u T_o}{(k_{\text{mix}} - 1) M_{M\text{mix}}} \left[1 - \left(\frac{p_e}{p_o} \right)^{(k-1)/k} \right]} \tag{1}$$

The preceding equation clearly shows that the exit velocity is inversely proportional to the square root of the molecular mass. Equation (1) also shows that the exit velocity is affected by the value of the mixture ratio of specific heats. Both the mixture molecular mass and the mixture ratio of specific heats will depend upon the composition of the exhaust gases, and thus, even without considering the Lorentz body force, the application of a magnetic field could impact nozzle exit velocity.

The impact of the Lorentz body force on conventional chemical rocket motors has been previously investigated.[4] The impact that a magnetic field has on rocket performance as a result of the paramagnetic and diamagnetic nature of the constituent gases alone has not previously been investigated. The goal of this investigation was to determine to what extent paramagnetism and diamagnetism affect theoretical rocket performance. The specific objectives of the study were as follows: 1) to develop a thermodynamic chemical equilibrium model that can be used to predict the changes in theoretical rocket performance for a chemical rocket in the presence of a uniform magnetic field considering only paramagnetic and diamagnetic effects; 2) to validate the thermodynamic model by comparison with existing chemical equilibrium and rocket performance models; 3) to examine the changes, caused by the application of a magnetic field, to parameters traditionally used to characterize rocket performance; and 4) to draw conclusions as to the relative impact that paramagnetism and diamagnetism have on rocket performance.

Formulation

To examine the impact a magnetic field has on theoretical rocket performance, the following assumptions have been made:

1) The exhaust consists of a mixture of ideal gases.

2) The composition of the exhaust gases is frozen throughout the nozzle.

3) The composition of the exhaust gases is the thermodynamic equilibrium composition at a state specified by the combustor pressure, the combustor temperature, and the applied magnetic field.

4) The equilibrium composition is that for the following model reaction of kerosene with oxygen:

$$\text{CH}_2 + a\text{O}_2 \rightarrow n_{\text{CO2}}\text{CO}_2 + n_{\text{H2O}}\text{H}_2\text{O} + n_{\text{CO}}\text{CO} + n_{\text{H2}}\text{H}_2 + n_{\text{OH}}\text{OH} + n_{\text{H}}\text{H} + + n_{\text{O2}}\text{O}_2 + + n_{\text{O}}\text{O} \tag{2}$$

5) The gases are expanded through a supersonic nozzle attached to an infinite area combustor.

6) The forces associated with the applied magnetic field are only paramagnetic and diamagnetic forces, that is, Lorentz forces are not considered.

7) The flow through the nozzle is isentropic.

8) The magnetic field is assumed to only affect the combustion process in the infinite area combustor.

As a result of the final assumption, defining the orientation of the magnetic field vector is not relevant. As shown next, the magnetic field is included in the equilibrium combustion model as a contribution to the work term in the First Law of Thermodynamics and as such does not explicitly include directional effects. The only paramagnetic species considered is diatomic oxygen. Because the magnetic susceptibility of oxygen is two orders of magnitude greater than that of the diamagnetic species, one is intuitively led to the conclusion that oxygen will play a critical role in determining the impact that a magnetic field will have on theoretical rocket performance. Recall that it has previously been stated that the magnetic susceptibility of paramagnetic gases is a function of temperature. In this effort, the magnetic susceptibility of diatomic oxygen has been assumed a constant as a result of the lack of information regarding the temperature dependence of oxygen's magnetic susceptibility. Although the assumption of frozen conditions tends to underestimate rocket performance, the assumption should not prevent an evaluation as to whether or not magnetic fields can influence rocket performance. It has also been assumed that the combustor is an infinite area combustor. As with the assumption of frozen conditions, the assumption of an infinite area combustor significantly simplified the analysis and should not prevent an evaluation as to whether or not a magnetic field can influence rocket performance as a result of paramagnetic and diamagnetic behavior.

From a thermodynamic point of view, paramagnetism and diamagnetism impact the First Law of Thermodynamics through the work contribution. The work contribution, including both boundary and magnetic field work, can be written as[8]

$$\delta W = -p\,\mathrm{d}V + \mathrm{d}\left(V \int H\,\mathrm{d}B \right) \tag{3}$$

Assuming the system consists of only diamagnetic and paramagnetic ideal gases, a modified expression for the Gibbs free energy of each component gas can be developed.[6] To find the equilibrium composition for a given chemical reaction at a specified state, the modified Gibbs free energy was minimized with respect to the conservation of mass constraint. This was achieved by the method of Lagrange multipliers, and details of the computational model can be found in Baker and Saito.[6] For the sake of brevity, the model used to generate the results presented in this paper will be referred to as the magneto-equilibrium combustion compositions (MECC) model. The algorithms for calculating theoretical rocket performance parameters are identical to those outlined in Gordon and McBride.[9]

A brief outline of the algorithm used to calculate the results presented in this paper is presented next for the sake of completeness:

1) The magnetic induction, oxygen-to-fuel ratio, stagnation pressure, stagnation temperature, and associated convergence tolerances are specified. A listing of these and other baseline parameters is presented in Table 1. Note that when not explicitly identified, the values in Table 1 are those used to generate the results.

2) The equilibrium composition in the infinite area combustor is calculated for the conditions specified in step 1. The mixture gas constant, the mixture constant pressure specific heat, the mixture ratio of specific heats, the mixture specific entropy, and the mixture specific enthalpy are calculated.

3) Assuming that the ratio of specific heats is constant and that the flow is isentropic, an initial estimate of the throat pressure and the throat temperature is calculated.

4) Using the estimates from step 3, the throat mixture specific entropy and the throat mixture constant-pressure specific heat are calculated. These values were used to calculate the natural log of the throat temperature via[9]

$$(\ell_n T_t)_{m+1} = (\ell_n T_t)_m + (\Delta\, \ell_n T_t)_m = (\ell_n T_t)_m + \frac{S_o - S_{t,m}}{c_{p,t,m}} \tag{4}$$

Using the results from Eq. (4), a new estimate of the throat temperature was calculated, and updated values of the throat mixture

Table 1 Baseline parameters

Parameter	Baseline value (s)
A_t	0.0001 m^2
B	0.0 T − 2.0 T
O/F	1.8, 2.3, 2.8
p_o	500 psia, 750 psia, 1000 psia
p_e	14.696 psia
T_o	3000 K, 3300 K, 3600 K

specific entropy and the throat mixture constant pressure specific heat were determined. These values were then used to calculate another estimate of the throat temperature. This process was continued until $|\Delta \ell_n T_t| < 1 \times 10^{-10}$.

5) Using the value of the throat temperature calculated in step 4, the throat mixture enthalpy, the throat ratio of specific heats, the throat pressure, the throat velocity, the throat density, and the throat mass flow rate were calculated.

6) A similar algorithm, that is, steps 3 and 4, was used to calculate the nozzle exit temperature. The exit pressure was specified in the model input. Using the calculated value of the exit temperature, the exit mixture enthalpy, the exit ratio of specific heats, the exit velocity, and the exit density were calculated.

7) Using the calculated values just mentioned, the mixture molecular mass was determined using

$$M_{M,\text{mix}} = \sum_{i=1}^{ns} y_i M_{M,i} \tag{5}$$

the specific impulse using

$$I_s = u_e/g \tag{6}$$

the thrust coefficient using

$$C_F = \dot{m} u_e / A_t P_o \tag{7}$$

and the expansion ratio using

$$A_e/A_t = \rho_t U_t / \rho_e u_e \tag{8}$$

Model Validation

To validate the results of the model developed during this investigation, the results for no applied magnetic field were compared to results from the chemical equilibrium analysis (CEA) model.[10] Although a wide range of conditions were examined to validate the MECC model, two sets of conditions are presented here for validation purposes:

Case 1:

$$p_o = 1000 \text{ psia}, \quad T_o = 4000 \text{ K}, \quad \text{and} \quad O/F = 3.0$$

Case 2:

$$p_o = 200 \text{ psia}, \quad T_o = 2600 \text{ K}, \quad \text{and} \quad O/F = 1.6$$

With regard to the chemical equilibrium compositions, the mole fraction percent difference ranges for the MECC model vs those using CEA are listed in Table 2. As can be seen from Table 2, the MECC results compare favorably with the results from CEA with the percent differences ranging from 0.0 to 1.74%. The differences are most likely the result of different convergence criteria for the equilibrium iterations. With regard to theoretical rocket performance, the specific impulse, the characteristic velocity, and the expansion ratio data from the MECC model were compared to results from the CEA model. Table 3 provides the results of this comparison. Again, the MECC results compare favorably with CEA results with the percent differences ranging from 0.024 to 0.38%. When an applied magnetic field was applied, the MECC model showed a trend toward an increasing OH mole fraction with an increasing magnetic induction. This trend qualitatively agrees with the physical measurements of Hayashi.[11] Based upon the preceding comparisons, the results from the MECC model are taken to be valid under the assumptions just mentioned.

Table 2 Validation results: equilibrium composition

Mole fraction	Percent different range, %
CO_2	0.33–0.84
CO	0.086–0.32
O	0.0
O_2	0.0
OH	1.5–2.47
H	0.0–0.8
H_2	0.12–1.74
H_2O	0.24–1.1

Table 3 Validation results: rocket performance

Parameter	Percent different range, %
I_S	0.035–0.088
c^*	0.024–0.030
A_e/A_t	0.069–0.38

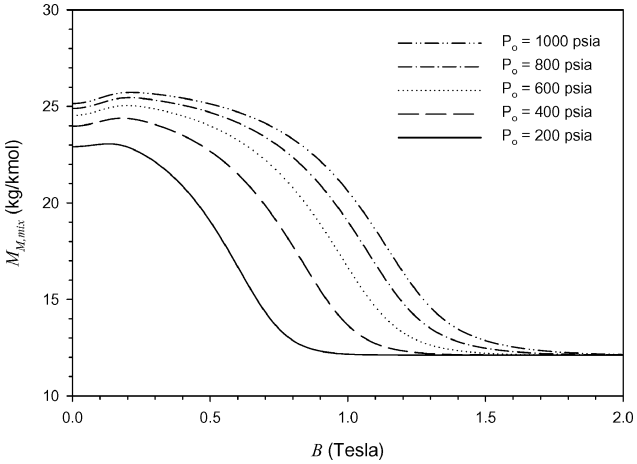

Fig. 1 Mixture molecular mass as a function of magnetic induction and stagnation pressure.

Results and Discussion

Figure 1 is a plot of the mixture molecular mass as a function of applied magnetic induction for various levels of chamber (stagnation) pressure. The molecular mass showed an initial increase for small values of the magnetic induction. This initial increase in molecular mass was more pronounced as the stagnation pressure was increased with a maximum increase in the mixture molecular mass of approximately 2.38% for the 1000-psia condition. The local maximum associated with this initial increase occurred for a magnetic induction 0.15 T at 200 psia and shifting toward values of larger magnetic induction as the pressure was increased. The local maximum occurred at a value of 0.25 T for a 1000-psia stagnation pressure.

Beyond this local maximum, the mixture molecular mass decreased for all stagnation pressures up to a certain saturation magnetic induction beyond which the value of the mixture molecular mass was no longer a function of magnetic induction. As with the local maximum, increases in the stagnation pressure increased the value of the saturation magnetic induction. The saturation magnetic induction was approximately 0.95 T for the 200-psia condition and increased to approximately 2.0 T for the 1000-psia condition. Beyond values of magnetic induction at or greater than the saturation magnetic induction, the decrease in mixture molecular mass relative to the mixture molecular mass with no applied magnetic field was approximately 46.49% for the 200-psia case and 51.59% for the 1000-psia case. Note also that beyond the saturation magnetic induction the mixture molecular mass was constant ($M_{M,\text{mix}} = 12.12$ kg/kmol) for all stagnation pressures considered.

Figure 2 is a plot of the mixture molecular mass as a function of applied magnetic induction for various levels of chamber (stagnation) temperature. As with the change in stagnation pressure, the application of a magnetic field initially increased the mixture molecular mass for the stagnation temperature considered. This increase was more pronounced for larger stagnation temperatures with a maximum change of approximately 2% for a 3700 K stagnation temperature. For the lowest two stagnation temperatures considered, no local maximum was observed. The value of the magnetic induction where the local maximum occurred slightly decreased with decreasing stagnation temperature. Beyond this local maximum, the mixture molecular mass decreased with increasing magnetic induction up to a certain saturation magnetic induction. This decrease,

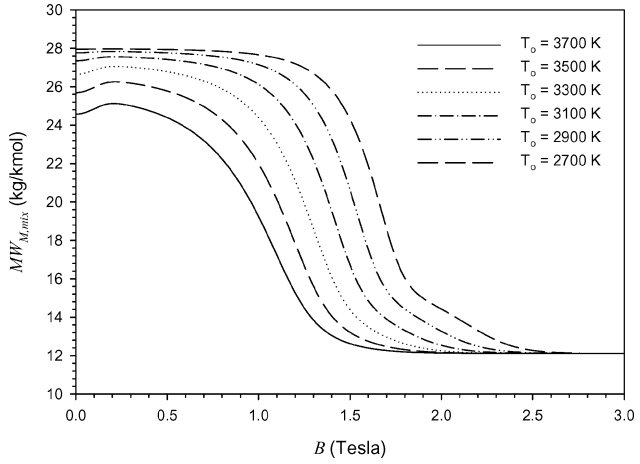

Fig. 2 Mixture molecular mass as a function of magnetic induction and stagnation temperature.

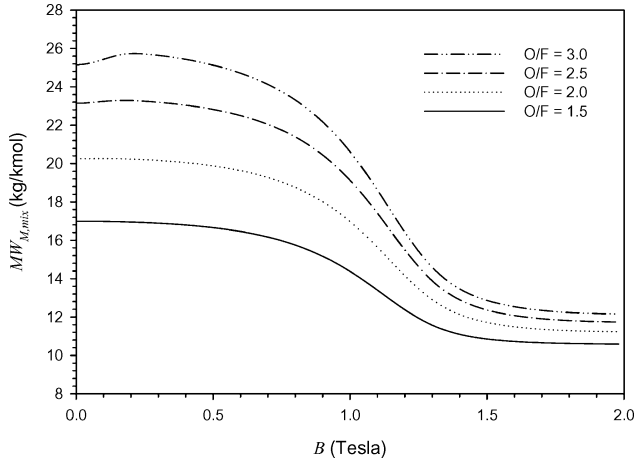

Fig. 3 Mixture molecular mass as a function of magnetic induction and oxygen-fuel ratio.

relative to the values with no applied magnetic field, was approximately 56.4% for a stagnation temperature of 2700 K and 50.4% for a stagnation temperature of 3700 K, that is, the impact of an applied magnetic field decreased with increasing temperature. The saturation magnetic induction increased with decreasing stagnation temperature with an approximate value of 2.7 T for a stagnation temperature of 2700 K and 1.8 T for a stagnation temperature of 3700 K. As in Fig. 1, the mixture molecular mass was a constant ($M_{M,\mathrm{mix}} = 12.12$ kg/kmol) above the saturation magnetic induction. In addition, once the saturation magnetic induction corresponding to a fixed stagnation temperature was reached the mixture molecular mass was again not a function of the stagnation temperature.

Figure 3 is a plot of the mixture molecular mass as a function of applied magnetic induction for various levels of the oxygen-fuel ratio. There is an increase in the mixture molecular mass for small values of the magnetic induction corresponding to an oxygen-fuel ratio of 2.5 and 3.0. For values of the oxygen-to-fuel ratio less than 2.5, a local maximum was not observed. The peak increase in mixture molecular mass was approximately 2% for the value of the oxygen-fuel ratio equal to 3.0. The value of the magnetic induction corresponding to this local maximum shifted to larger values for increased oxygen-fuel ratios. As with the other cases, the application of a magnetic field of sufficient strength caused a significant decrease in the mixture molecular mass up to the saturation magnetic induction. Relative to values with no applied magnetic field, the application of a magnetic field caused the mixture molecular mass to decrease by approximately 38.2% for the $O/F = 1.5$ and 52.4% for $O/F = 3.0$. Beyond the saturation magnetic induction, the mixture molecular mass was constant with respect to magnetic induction for a given oxygen-fuel ratio. Note that the mixture molecular mass is a function of the oxygen-fuel ratio above the saturation magnetic induction, but the dependence of the mixture molecular mass on oxygen-fuel ratio is decreased with the application of a magnetic field. Beyond the saturation magnetic induction, the percent change in the mixture molecular mass was approximately 14.3% for the range of oxygen-fuel ratios considered. With no applied magnetic field, the percent change in the mixture molecular mass associated with a change in the oxygen-fuel ratio from 1.5 to 3.0 was 48.2%.

Figures 4–6 are plots of the expansion ratio as a function of magnetic induction for various chamber (stagnation) pressures, chamber (stagnation) temperatures, and oxygen-fuel ratios. Recall that the throat area is fixed for the model developed during this study and that the nozzle exit area is calculated as that necessary to maintain isentropic flow throughout the nozzle. For small applied magnetic inductions, there was a slight increase in the expansion ratio for the larger stagnation pressures and temperatures as well as for the largest oxygen-fuel ratio considered. After achieving a local maximum, the expansion ratio decreased as a function of applied magnetic induction to some saturation magnetic induction value beyond which an increase in magnetic induction had no effect. This saturation magnetic induction increased with stagnation pressure, stagnation temperature, and oxygen-fuel ratio. With regard to stagnation pressure, the percent decrease in expansion ratio relative to the expansion ratio when no magnetic field was applied was 39.5 and 20.4% for stagnation pressures of 1000 and 200 psia, respectively. With regard to stagnation temperature, once the saturation magnetic induction had been reached, the expansion ratio was only a weak function of stagnation temperature. Beyond the saturation magnetic induction, the functional behavior of the expansion ratio with regard to the stagnation temperature also changed with the expansion

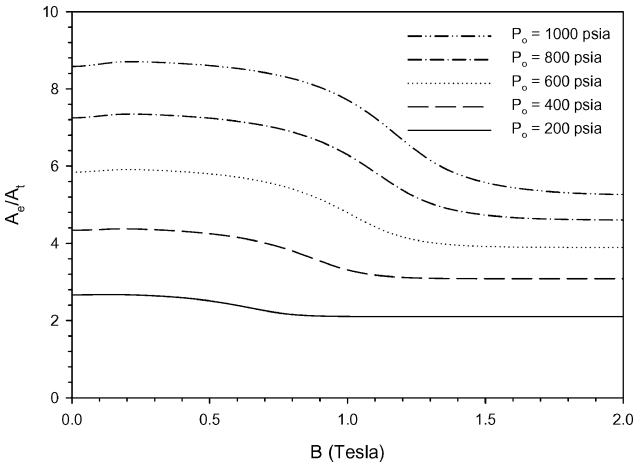

Fig. 4 Expansion ratio as a function of magnetic induction and stagnation pressure.

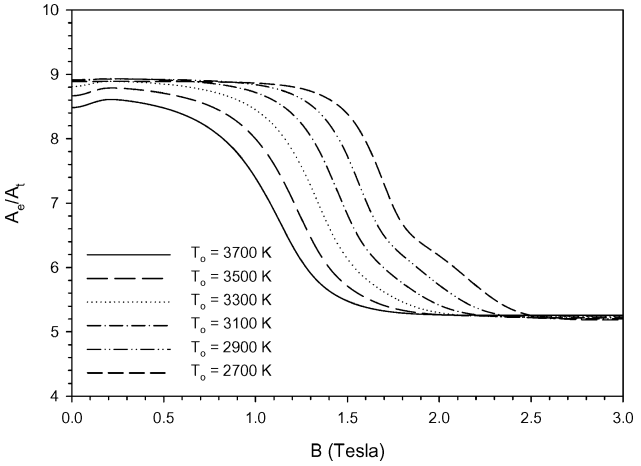

Fig. 5 Expansion ratio as a function of magnetic induction and stagnation temperature.

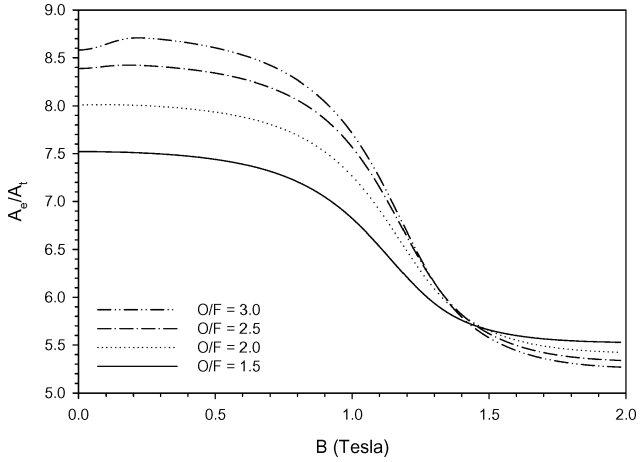

Fig. 6 Expansion ratio as a function of magnetic induction and oxygen-fuel ratio.

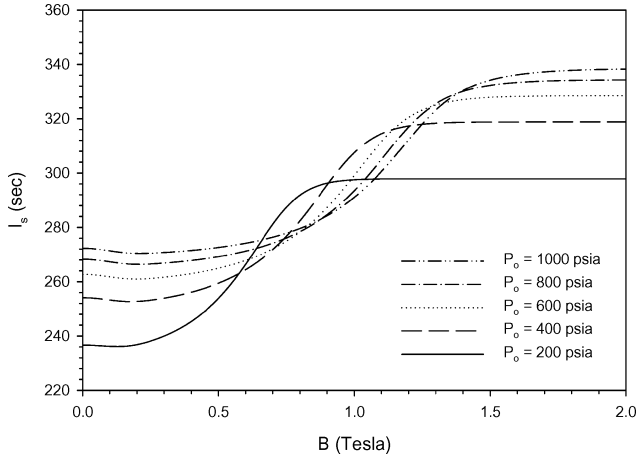

Fig. 7 Specific impulse as a function of magnetic induction and stagnation pressure.

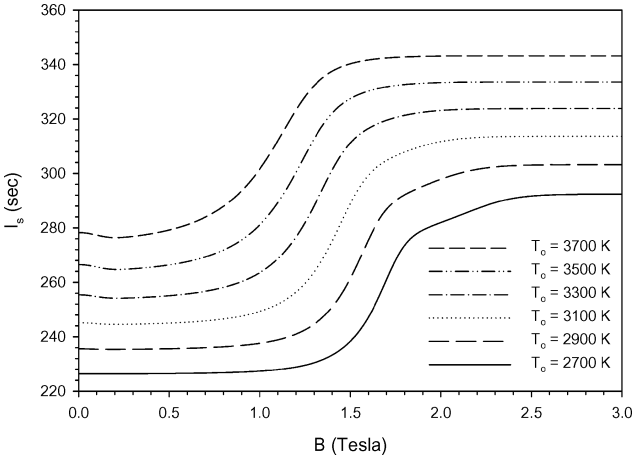

Fig. 8 Specific impulse as a function of magnetic induction and stagnation temperature.

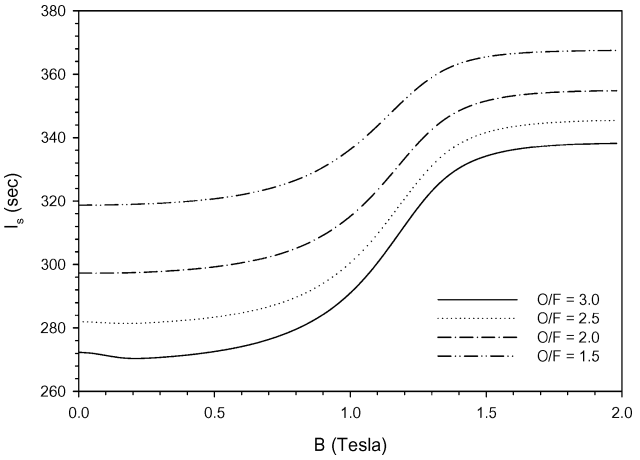

Fig. 9 Specific impulse as a function of magnetic induction and oxygen-fuel ratio.

ratio increasing with increasing temperature. This sort of change in behavior is more pronounced when considering the expansion ratio as a function of magnetic induction for various oxygen-fuel ratios. As can be seen from Fig. 6, beyond a magnetic induction of approximately 1.45 the expansion ratio decreases with increasing oxygen-fuel ratio up to the saturation magnetic induction. As the oxygen-fuel ratio increased, the influence of an applied magnetic field on the expansion ratio increased. This was expected given the magnitude of the paramagnetic oxygen's magnetic susceptibility relative to that of the diamagnetic fuel and combustion products.

Figures 7–9 are plots of the specific impulse as a function of magnetic induction for various chamber (stagnation) pressures, chamber (stagnation) temperatures, and oxygen-fuel ratios. For all of the cases, the application of a relatively small magnetic field caused a slight decrease in the specific impulse. For larger applied magnetic fields, an applied magnetic field increased the specific impulse. With regard to stagnation pressure, this overall increase relative to the specific impulse with no applied magnetic field was on the order of 25% with the percent change increasing for decreasing stagnation pressure. For stagnation temperature, the percent increase in specific impulse varied from approximately 29% at a stagnation temperature of 2700 K to a value of approximately 23% at a stagnation temperature of 3700 K. For oxygen-fuel ratio, the percent increase in specific impulse decreased with increasing oxygen-fuel ratio from a value of approximately 24% for an oxygen-fuel ratio of 1.5 to approximately 15% for an oxygen-fuel ratio of 3.0. The existence of a saturation value for the magnetic induction can also be observed in Figs. 7 and 8. This saturation magnetic induction value ranged from 1.48 T at a stagnation pressure of 200 psia to a value of 2.51 T at a stagnation pressure of 1000 psia. With regard to stagnation temperature, the saturation magnetic induction ranged from 2.76 T at a stagnation temperature of 2700 K to 2.46 T at a stagnation temperature of 3700 K. Although Fig. 9 seems to indicate that a magnetic saturation value also exists for the different oxygen-fuel ratios, a close examination of the data shows that even at 2 T there is still a slight increase in the specific impulse with increasing magnetic induction. The reason for the specific impulse behavior can be easily explained by examining the molecular mass data discussed earlier. As the molecular mass decreases with increasing magnetic induction, the associated exit velocity increases, and thus the specific impulse increases.

Figures 10–12 are plots of the thrust coefficient as a function of magnetic induction for various chamber (stagnation) pressures, chamber (stagnation) temperatures, and O/F ratios. As can be seen in the plots for small applied magnetic fields, the thrust coefficient was constant or showed a slight increase. This increase was most pronounced for the case of an oxygen-fuel ratio of 3.0. As with the expansion ratio, the application of an applied magnetic field of sufficient strength decreased the thrust coefficient. With regard to stagnation pressure, the decrease was on the order of 1.5% for the 200-psia case and increased to approximately 6.3% for the 1000-psia case for a magnetic field at or above the saturation magnetic induction value. With regard to stagnation temperature, the influence of the applied magnetic field on the thrust coefficient decreased with increasing temperature. The decrease in the thrust coefficient ranged from 6.4% at a stagnation temperature of 3700 K to 7.3% at a stagnation temperature of 2700 K. From Figs. 10 and 11, a saturation magnetic induction beyond which the thrust coefficient is constant was observed. In terms of stagnation pressure, this saturation magnetic induction ranged from 0.99 T at 200 psia to 2.39 T at 1000 psia.

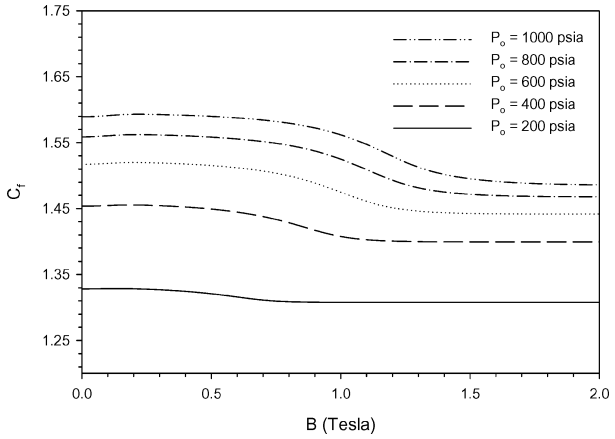

Fig. 10 Thrust coefficient as a function of magnetic induction and stagnation pressure.

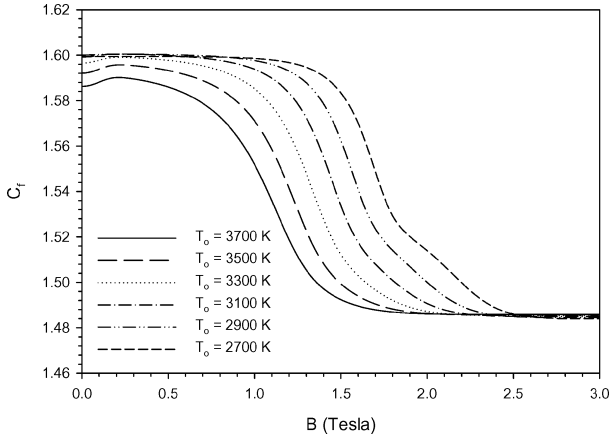

Fig. 11 Thrust coefficient as a function of magnetic induction and stagnation temperature.

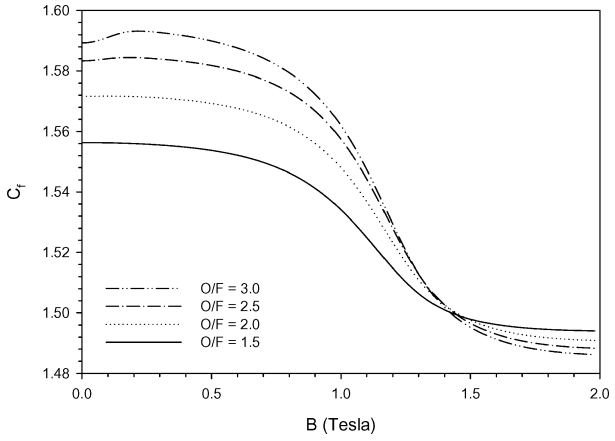

Fig. 12 Thrust coefficient as a function of magnetic induction and oxygen-fuel ratio.

In contrast, an increase in stagnation temperature decreased the saturation magnetic induction. For a stagnation temperature of 2700 K, the saturation magnetic induction was 2.76 T, and for a stagnation temperature of 3700 K the saturation magnetic induction was 2.15 T. With regard to the oxygen-fuel ratio, no saturation value was observed in the range of magnetic induction considered. From Figs. 11 and 12, a critical value of the magnetic induction was observed above which the functional relationship for the thrust coefficient changed. Above a value of magnetic induction of approximately 2.5 T, an increase in stagnation temperature slightly decreased the thrust coefficient. For a magnetic induction above approximately 1.45 T, a decrease in oxygen-fuel ratio increased thrust coefficient. The reason for this behavior is not clear. The fact that the application of a magnetic field decreased the thrust coefficient was initially surprising, given the molecular mass and specific impulse behavior already discussed. To explain this decrease, it is necessary to examine the definition of the thrust coefficient. For the problem examined here, the throat area and the stagnation pressure are fixed. From the specific impulse data it is known that the exit velocity increases with the application of a magnetic field.

Therefore, to obtain such a decrease in the thrust coefficient there must be a more pronounced decrease in the product of the exit density times the exit area. Recall that the application of an applied magnetic field resulted in a decrease in the exit area in order to maintain isentropic flow conditions. The result might also imply that there is a decrease in mixture density with the application of a magnetic field of sufficient strength. From this discussion, it is possible to conclude that while the application of the magnetic field does increase specific impulse changes in the state of the gases as a result of the magnetic field decrease the thrust of an engine.

Conclusions

A computational model has been used to examine the impact an applied magnetic field has on theoretical rocket performance. The model calculated the chemical equilibrium composition of a kerosene-oxygen mixture at specified conditions and assumed frozen behavior throughout the supersonic nozzle. Based upon the results of this study, the following conclusions have been drawn:

1) The application of a magnetic field decreased the mixture molecular mass, decreased the expansion ratio required to maintain isentropic flow conditions, increased specific impulse, and decreased the thrust coefficient.

2) For most of the scenarios considered, a saturation magnetic induction existed beyond which an increase in the magnetic induction had no impact on rocket performance.

3) A critical magnetic induction existed beyond which the functional behavior of the expansion ratio and the thrust coefficient change. This change was slight with respect to stagnation temperature, significant with respect to the oxygen-fuel ratio, and was not observed with respect to variations in the stagnation pressure.

4) Applying a magnetic field to the combustion chamber of a chemical rocket does significantly influence theoretical rocket performance via the paramagnetic and diamagnetic nature of the constituent gases. Additional investigation is needed to quantify this impact in an actual chemical rocket.

References

[1]Nagamine, Y., and Nakashima, H., "Analysis of Plasma Behavior in a Magnetic Thrust Chamber of a Laser Fusion Rocket," *Fusion Technology*, Vol. 35, No. 1, 1999, pp. 62–70.

[2]Santarius, J. F., and Logan, G. B., "Generic Magnetic Fusion Rocket Engine," *Journal of Propulsion and Power*, Vol. 14, No. 4, 1998, pp. 519–524.

[3]Sasoh, A., and Arakawa, Y., "Electromagnetic Effects in an Applied-Field Magnetoplasmadynamic Thruster," *Journal of Propulsion and Power*, Vol. 8, No. 1, 1992, pp. 98–102.

[4]Borovskoi, I. G., and Vorozhtsov, A. B., "Magnetic Field Control of Burning Rate and Thrust in Solid Rocket Motors," *Journal of Propulsion and Power*, Vol. 11, No. 4, 1995, pp. 824–829.

[5]Borovskoi, I. G., Vorozhtsov, A. B., and Salko, A. E., "Magnetogasdynamic Control of Burning Rate of Condensed System," *Defense Science Journal*, Vol. 45, No. 1, 1995, pp. 47–49.

[6]Baker, J., and Saito, K., "Magnetocombustion: A Thermodynamics Analysis," *Journal of Propulsion and Power*, Vol. 16, No. 2, 2000, pp. 263–268.

[7]Sutton, G. P., and Biblarz, O., *Rocket Propulsion Elements*, 7th ed., Wiley-Interscience, New York, 2001, p. 52.

[8]Rosenwieg, R. E., *Ferrohydrodynamics*, Cambridge Univ. Press, New York, 1985, p. 101.

[9]Gordon, S., and McBride, B. J., "Computer Program for Calculation of Complex Chemical Equilibrium Compositions and Applications. I. Analysis," NASA RP 1311, June 1996.

[10]Gordon, S., and McBride, B. J., "Computer Program for Calculation of Complex Chemical Equilibrium Compositions and Applications. II. Users Manual and Program Description," NASA RP 1311, Oct. 1994.

[11]Hayashi, H., "The External Magnetic Field Effect on the Emission Intensity of the A2$\Sigma+ \rightarrow$ X2Π (O-O) Transition of the OH Radical in Flames," *Chemical Physics Letters*, Vol. 87, No. 2, 1982, pp. 113–116.